

Imaging polarimetry of the fogbow: polarization characteristics of white rainbows measured in the high Arctic

Gábor Horváth,^{1,*} Ramón Hegedüs,^{2,6} András Barta,^{1,4}
Alexandra Farkas,^{1,5} and Susanne Åkesson^{3,7}

¹Environmental Optics Laboratory, Department of Biological Physics, Physical Institute, Eötvös University, H-1117 Budapest, Pázmány sétány 1, Hungary

²Computer Vision and Robotics Group, University of Girona, Campus de Montilivi, Edifici P4, 17071 Girona, Spain

³Department of Biology, Centre for Animal Movement Research, Lund University, Ecology Building, SE-223 62 Lund, Sweden

⁴e-mail: bartaandras@gmail.com

⁵e-mail: farkasalexandra@upcmil.hu

⁶e-mail: ramon.hegedus@gmail.com

⁷e-mail: susanne.akesson@biol.lu.se

*Corresponding author: gh@arago.elte.hu

Received 25 May 2011; accepted 26 July 2011;
posted 5 August 2011 (Doc. ID 148177); published 12 September 2011

The knowledge on the optics of fogbows is scarce, and their polarization characteristics have never been measured to our knowledge. To fill this gap we measured the polarization features of 16 fogbows during the Beringia 2005 Arctic polar research expedition by imaging polarimetry in the red, green and blue spectral ranges. We present here the first polarization patterns of the fogbow. In the patterns of the degree of linear polarization p , fogbows and their supernumerary bows are best visible in the red spectral range due to the least dilution of fogbow light by light scattered in air. In the patterns of the angle of polarization α fogbows are practically not discernible because their α -pattern is the same as that of the sky: the direction of polarization is perpendicular to the plane of scattering and is parallel to the arc of the bow, independently of the wavelength. Fogbows and their supernumeraries were best seen in the patterns of the polarized radiance. In these patterns the angular distance δ between the peaks of the primary and the first supernumerary and the angular width σ of the primary bow were determined along different radii from the center of the bow. δ ranged between 6.08° and 13.41° , while σ changed from 5.25° to 19.47° . Certain fogbows were relatively homogeneous, meaning small variations of δ and σ along their bows. Other fogbows were heterogeneous, possessing quite variable δ - and σ -values along their bows. This variability could be a consequence of the characteristics of the high Arctic with open waters within the ice shield resulting in the spatiotemporal change of the droplet size within the fog. © 2011 Optical Society of America

OCIS codes: 010.1290, 110.5405.

1. Introduction

One of the most spectacular atmospheric optical phenomena is the rainbow occurring when sunlight is

reflected from water droplets falling in the air [1–5]. The physics of rainbows is well understood and a large amount of knowledge has been accumulated in the last century [6–13]. Among others, the polarization characteristics of the rainbow have also been studied theoretically [14–16] and experimentally [17,18].

A special type of the rainbow phenomenon is the fogbow, also called Ulloa’s ring, Bouguer’s halo, mistbow or white rainbow [19–22], when sunlight is reflected (back-scattered) from tiny water droplets levitating (slowly sedimenting) in the air. The emergent sunlight is mostly deviated by 135° to 150° from its incident direction to produce the main fogbow of 30° – 45° radius centered on the antisolar point. The deviation corresponds roughly to the geometric optics angle of minimum deviation of $\sim 138^\circ$ for the 42° radius rainbow [1,4,23]. The first observation reported as a written account was made in 1735 by Ulloa and Juan from Mount Pambamarca in the present-day Ecuador [22]. Lee and Fraser [5] also presented several older documentations from Theodoric, Avicenna and Witelo, but the phenomenon was misinterpreted in these old descriptions. While Theodoric correctly noted that the primary rainbow and fogbow arose in the same way, he offered no convincing explanation as to why their colors differed. Avicenna explained that the diameter of his cloud-bow was reduced because he grew more distant from the sun as he descended the mountain toward the bow. Witelo simply regarded the white rainbow as a combination of thin vapor and clear illumination. According to Hunter [24], Horace Benedict de Saussure put forward a theory that in fog the floating droplets of water are small hollow spheres. The French scientist August Bravais followed de Saussure in holding this theory. Tyndall [19] sought for these hollow spheres but could not find them, and he had no difficulty in disproving their existence. According to Lynch and Schwartz [25], the unusual appearance of the fogbow is correctly attributed to its origin in small droplets, the radii of which are less than $\sim 50\ \mu\text{m}$, and thus diffract light strongly.

The optical characteristics of the fogbow depend on the size of the fog droplets. Because of the small droplet size the differently colored arcs overlap considerably, therefore the bright fogbow is white. The reported mean drop radius is always smaller than $60\ \mu\text{m}$, and usually ranges from 25 to $50\ \mu\text{m}$. According to Lynch and Schwartz [25], the fogbows are paler and more faded for drops smaller than $50\ \mu\text{m}$, and will exhibit colors if drops are larger than $\sim 100\ \mu\text{m}$. As the droplet diameter increases, the primary bow narrows and the supernumerary bows inside the main bow move close together (Fig. 1). Cowley [23] found that these supernumerary bows are produced by the constructive and destructive interference of overlapping wave crests along the main light path.

The fogbow occurs more rarely than the rainbow; thus its optics have only scarcely been studied. The polarization of fogbow light has been demonstrated

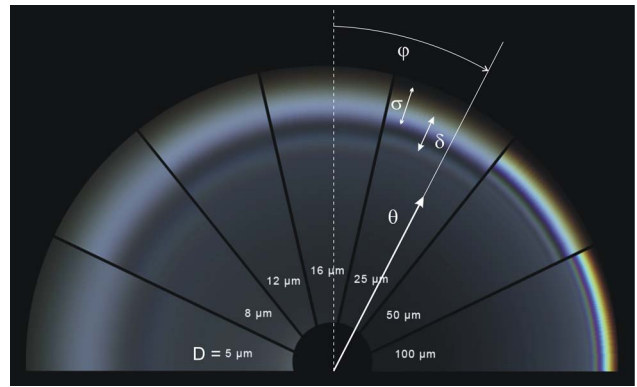


Fig. 1. (Color online) Simulated appearance of the fogbow as a function of the droplet diameter D ranging from 5 to $100\ \mu\text{m}$. The fogbow patterns were computed by the software IRIS (© Les Cowley [23], <http://atoptics.co.uk>). φ : angle (clockwise from the vertical) of the direction of a given radius. δ : angular distance between the peaks of the primary bow and the first supernumerary bow. σ : angular width of the primary bow. θ : angular distance from the bow center along a radius.

with photographs taken through linear polarizers [26,27]. According to Können [15], the degree of linear polarization of the fogbow is lower than that of the rainbow; therefore the fogbow usually cannot be totally extinguished with a linearly polarizing filter. The polarization characteristics of fogbows have never been quantitatively measured. To fill this gap, using imaging polarimetry, we measured the polarization features of several fogbows during the Beringia 2005 Arctic polar research expedition in the red, green, and blue parts of the spectrum. We present here the first polarization patterns of the fogbow, which can also inspire future theoretical and computational studies in this topic.

2. Materials and Methods

The polarization characteristics of fogbows were measured by imaging polarimetry between 25 August and 20 September 2005 at different locations during the third part (Leg 3) of the Beringia 2005 international Arctic polar research expedition organized by the Swedish Polar Research Secretariat. The expedition crossed the Arctic Ocean with the Swedish icebreaker research vessel, the Oden (departing from Barrow, $71^\circ 17' \text{N}$, $156^\circ 47' \text{W}$, Alaska and arriving in Longyearbyen, $78^\circ 12' \text{N}$, $15^\circ 49' \text{W}$, island of Spitsbergen, Svalbard, Norway). The method of imaging polarimetry has been described in detail elsewhere [18,28–31]. In our polarimeter we used a 180° field-of-view fisheye lens (Nikon-Nikkor, $F = 2.8$, focal length 8 mm) with a built-in rotating disc mounted with three broadband (275–750 nm) neutral density linearly polarizing filters (Polaroid HNP'B) with three different polarization axes (0° , 45° and 90° from the radius of the disc). The detector was a photo emulsion (Kodak Elite Chrome ED 200 ASA color reversal film; the maxima and half-bandwidths of its spectral sensitivity curves were $\lambda_{\text{red}} = 650 \pm 40\ \text{nm}$, $\lambda_{\text{green}} = 550 \pm 40\ \text{nm}$,

$\lambda_{\text{blue}} = 450 \pm 40 \text{ nm}$) in a roll-film photographic camera (Nikon F801). For a given fogbow three photographs were taken for the three different directions of the transmission axis of the polarizers. The camera was set on a tripod such that the optical axis of the fisheye lens was nearly horizontal or pointed to the center of the fogbow. After 24 bit (3×8 for red, green and blue) digitization (by a Canon Arcus 1200 scanner) of the three chemically developed color slides for a given fogbow and their computer evaluation, the patterns of the radiance I , degree of linear polarization p and angle of polarization α (measured clockwise from the vertical) of skylight and fogbow light were determined as color-coded, two-dimensional, circular maps, in which the center was on the horizon or coincided approximately with the center of the fogbow, and the angle from the center θ is proportional to the radius from the center (center: $\theta = 0^\circ$, circular perimeter: $\theta = 90^\circ$) [Fig. 1]. These patterns were obtained in the red, green, and blue spectral ranges, in which the three color-sensitive layers of the photo emulsion used have maximal sensitivity.

The angular distance δ between the peaks of the primary and the first supernumerary bow, and the angular width σ of the primary bow (Fig. 1, Table 1) were determined from the pattern of the polarized radiance $PI = p \cdot I$ (where I is the radiance, and p is the degree of linear polarization) measured in the red spectral range, since the disturbing light scattering between the polarimeter and the fogbow as well as behind the fog is the weakest in the red part of the spectrum. The original PI patterns were quite noisy. Thus a smoothed version of each PI pattern was created by replacing the polarized radiance value in each pixel with the value averaged on its $20 \text{ pixel} \times 20 \text{ pixel}$ neighboring area, the center of which was the given pixel. In this smoothed PI pattern the center of the fogbow was determined by fitting a circle on the primary bow. Then, the curve of polarized radiance of the fogbow was obtained along a given radius of the fogbow. The angular distance δ between the peaks of the primary bow and the first supernumerary bow was determined as the angle between the maxima of PI of the primary bow and of the first supernumerary bow along the investigated radius. The angular width σ of the primary bow was determined as the angle between the two local minima of PI around the PI maximum of the primary bow along a given radius.

3. Results

Figure 2 shows the color picture, polarized radiance $PI = p \cdot I$, and the patterns of the radiance I , degree of linear polarization p and angle of polarization α of an Arctic fogbow measured by imaging polarimetry in the red, green, and blue parts of the spectrum. In the color picture [Fig. 2(a)] the almost full circle of the white fogbow can be well seen, and the first supernumerary bow is also slightly visible. The background of the upper and lower parts of the fogbow is

Table 1. Angular Distance δ between Peaks of Primary Bow and First Supernumerary Bow, and Angular Width σ of Primary Bow of Arctic Fogbows Measured by Imaging Polarimetry Along Different Radii (from Center of Bow), the Direction φ of Which Is Measured Clockwise from the Vertical

Radial Direction φ	Angular Distance δ of Peaks	Angular Width σ of Bow
Fogbow 1		
0°	10.0°	14.51°
30°	9.47°	15.04°
-30°	8.93°	14.37°
Fogbow 2		
0°	6.36°	14.13°
30°	8.17°	12.39°
-30°	11.65°	15.40°
Fogbow 3		
0°	7.90°	16.94°
30°	—	10.31°
Fogbow 4		
0°	6.61°	13.29°
30°	7.95°	14.29°
60°	7.48°	14.09°
-60°	6.74°	15.49°
-30°	7.68°	16.69°
Fogbow 5		
0°	8.10°	13.53°
30°	8.10°	15.80°
60°	8.57°	13.79°
-60°	9.04°	15.94°
-30°	8.64°	12.25°
Fogbow 6		
0°	—	16.54°
30°	6.90°	15.67°
60°	7.70°	16.27°
-60°	7.37°	14.33°
-30°	—	15.33°
Fogbow 7		
0°	6.26°	10.84°
60°	7.47°	17.97°
-60°	7.88°	12.52°
-30°	6.93°	—
Fogbow 8		
60°	7.34°	16.56°
-60°	7.55°	18.76°
-30°	6.08°	14.89°
Fogbow 9		
0°	7.00°	12.86°
30°	7.67°	11.71°
-60°	7.40°	11.78°
-30°	6.73°	13.46°
Fogbow 10		
0°	7.74°	17.17°
30°	9.76°	—
60°	6.80°	15.28°
-60°	7.40°	16.96°
-30°	10.84°	18.98°
Fogbow 11		
0°	10.85°	14.48°
30°	8.02°	13.61°
60°	13.41°	14.08°
-60°	8.02°	16.17°
-30°	9.16°	19.47°
Fogbow 12		
0°	9.16°	12.87°
30°	7.48°	8.96°
60°	7.88°	15.49°

(Table continued)

Table 1. (Continued)

Radial Direction φ	Angular Distance δ of Peaks	Angular Width σ of Bow
-60°	7.81°	16.57°
-30°	7.81°	15.29°
Fogbow 13		
0°	6.39°	16.49°
30°	8.82°	14.81°
-60°	9.29°	16.36°
-30°	9.29°	15.08°
Fogbow 14		
0°	6.66°	12.52°
30°	6.26°	8.95°
60°	6.60°	14.47°
-60°	6.13°	9.90°
-30°	8.01°	14.88°
Fogbow 15		
30°	12.05°	13.40°
60°	6.80°	15.89°
-60°	6.60°	5.25°
-30°	9.56°	14.34°
Fogbow 16		
0°	6.33°	14.35°
30°	6.94°	10.85°
60°	6.33°	11.65°
-60°	7.14°	9.97°
-30°	7.54°	10.24°

the blue sky and the dark sea surface, respectively. The topmost part of the bow is almost invisible due to the low density of the fog there: where the fog is thin, the radiance of back-scattered fogbow light is low and overwhelmed by the more intense skylight from the background and foreground. The fogbow is best visible in the red radiance pattern [Fig. 2(c)] and least visible in the blue radiance pattern [Fig. 2(e)] because the blue skylight is least intense in the red and most intense in the blue. As the wavelength λ decreases the radiance of the fogbow is progressively overwhelmed by the skylight, the radiance of which increases with decreasing λ . The consequence of this is that the fogbow is almost indiscernible in the blue part of the spectrum [Fig. 2(e)].

On the other hand, both the primary fogbow and its first supernumerary bow are well visible in the pattern of polarized radiance PI [Fig. 2(b)]. In the PI pattern the fogbow is clearly seen even at its topmost part, contrary to that in the color picture [Fig. 2(a)] or the radiance patterns [Fig. 2(c)–2(e)]. The reason for this is that PI is the multiplication of the degree of linear polarization p and the radiance I , and where I is small, p can be high, as at the topmost part of the fogbow. Although the radiance I is relatively large in the red, green, and blue parts of the spectrum between the sea horizon and the upper half of the fogbow [Fig. 2(c)–2(e)], this half circular area is quite dark in the PI pattern because there the degree of polarization is practically zero ($p \approx 0$) in all three spectral ranges [Fig. 2(f)–2(h)]. In the PI pattern, the region between the sea horizon and the lower half of the fogbow is relatively bright in spite of the rather

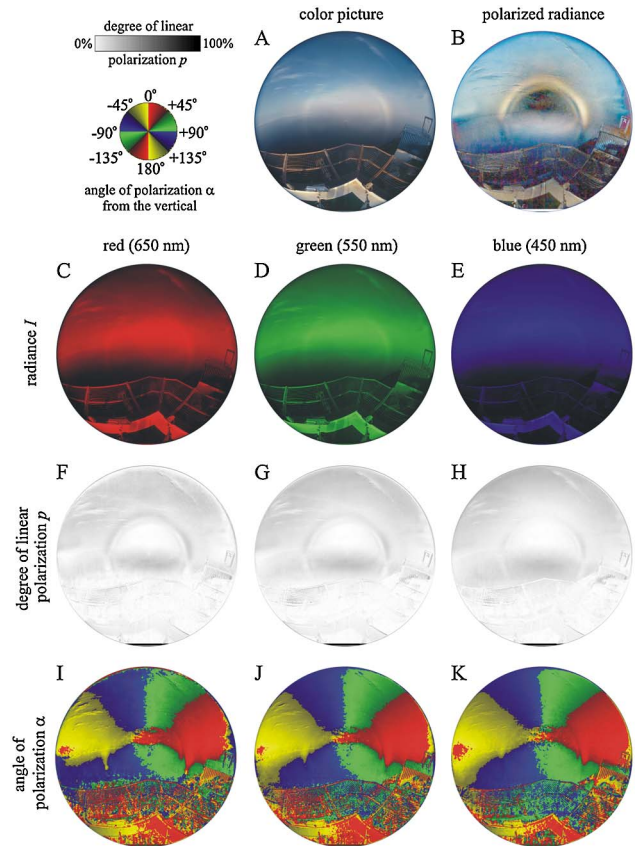


Fig. 2. (Color online) Color picture (A), polarized radiance $PI = p \cdot I$ (B), and patterns of the radiance I (C)–(E), degree of linear polarization p (F)–(H) and angle of polarization α (I)–(K) of an Arctic fogbow measured by imaging polarimetry in the red, green, and blue parts of the spectrum. Angle α is measured clockwise from the vertical. Figure b is a composite image of the polarized radiance PI : in the red, green, and blue channels the PI values measured in the red, green, and blue spectral ranges, respectively, are displayed.

low radiance of the sea surface [Fig. 2(c)–2(e)]. The reason for this is that the p of light reflected from the sea surface is high [Fig. 2(f)–2(h)]. The sky is bright blue in the PI pattern because I is relatively high in all three parts of the spectrum, and I is largest in the blue [Fig. 2(c)–2(e)].

Figure 3 shows the change of the degree of linear polarization p as a function of the angular distance θ from the center of the bow measured along five different radii of the fogbow in Fig. 2 in the red, green, and blue parts of the spectrum. In Fig. 3 both the primary bow and the first supernumerary bow are clearly seen. The degree of linear polarization p of the fogbow light decreases with decreasing wavelength, and more or less changes along the bow. In the patterns of the angle of polarization α [Fig. 2(i)–2(k)] we can see that the directions of polarization of the fogbow and its first supernumerary are the same as those of the sky: the direction of polarization is perpendicular to the plane of scattering and is parallel to the arc of the bow. The α pattern is practically independent of the wavelength of light.

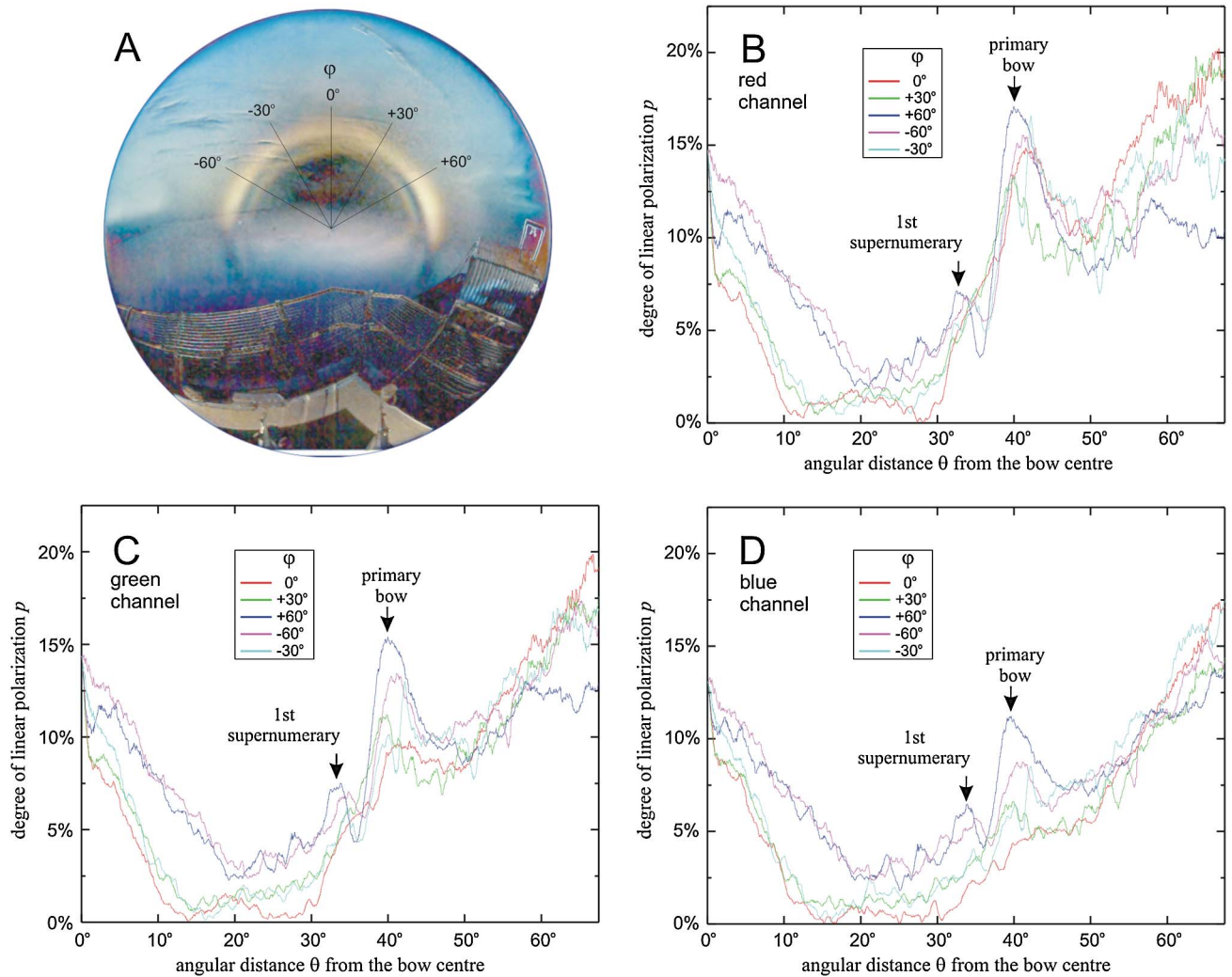


Fig. 3. (Color online) (A) Directions $\varphi = -60^\circ, -30^\circ, 0^\circ, +30^\circ, +60^\circ$ of the radii from the bow center, along which the data in Figs. 3–5 are measured. (B)–(D) Change of the degree of linear polarization p as a function of the angular distance θ from the center of the bow measured along five different radii (from the center of the bow) of the fogbow in Fig. 2 in the red (B), green (C), and blue (D) parts of the spectrum. The directions φ (clockwise from the vertical) of the radii are given in the inset.

We measured the polarization characteristics of 16 fogbows in the high Arctic, the polarization patterns of which were similar to those of the fogbow in Fig. 2. Table 1 contains the angular distances δ between the peaks of the primary and the first supernumerary bow, and the angular widths σ of the primary bow of these fogbows measured along different radii from the center of the bow. δ ranged between 6.08° (fogbow 8) and 13.41° (fogbow 11), while σ changed from 5.28° (fogbow 15) to 19.47° (fogbow 11). Fogbows 4, 9, and 16, for example, were relatively homogeneous, meaning small variations of δ and σ along their bows. On the other hand, fogbows 2, 11, and 15, for instance, were heterogeneous, possessing quite variable values of δ and σ along their bows.

Figure 4 shows two examples of fogbows whose polarized radiance PI , angular peak distance δ and angular bow width σ changed only moderately along the bow. Figure 5 gives two examples of fogbows, along the bow of which PI , δ and σ substantially

changed. In Fig. 6, six selected fogbows were compared with each other in the pattern of polarized radiance in a similar way as in Fig. 1.

4. Discussion

In the patterns of the degree of linear polarization p of Fig. 2 as well as in Fig. 3, the fogbow is best seen in the red spectral range because p of light from the fogbow is highest in this part of the visible spectrum. The reason for this is that p of the fogbow light is reduced by (i) the skylight coming from the background and (ii) the light scattered in the air between the fog and the observer (foreground). Both scattered components show the highest and lowest intensity in the blue and red spectral range, respectively, due to the $1/\lambda^4$ law of Rayleigh scattering. Hence, the polarized fogbow light is the least diluted by scattered light in the red part of the spectrum, and thus its net p is highest in this spectral range. Furthermore, both Rayleigh scattered components are almost

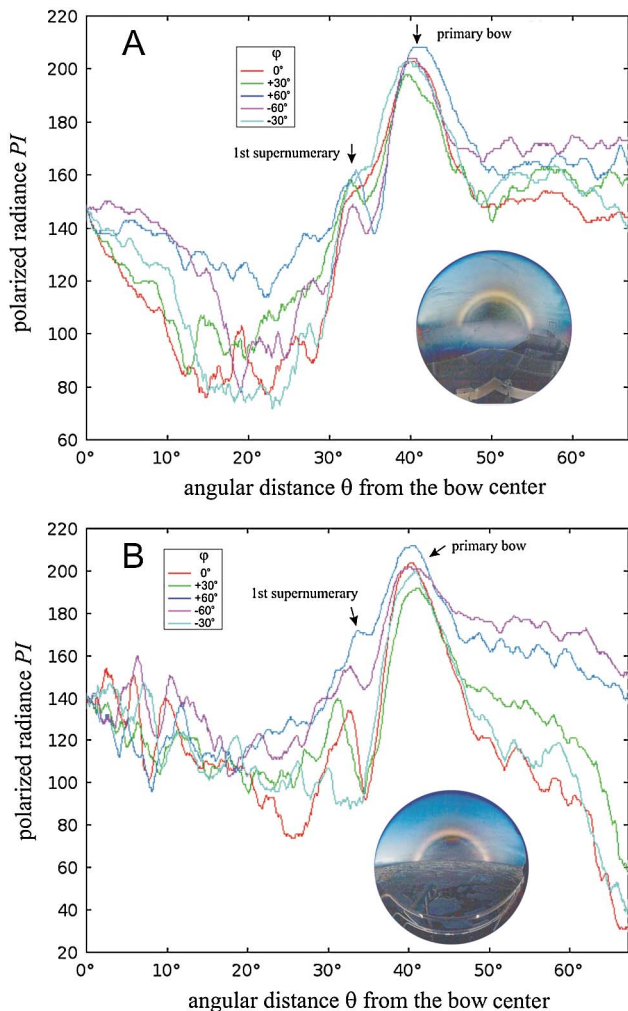


Fig. 4. (Color online) Change of the polarized radiance PI (in relative units) as a function of the angular distance θ from the center of the bow measured along five different radii (from the center of the bow) of the Arctic fogbows 6 (A) and 10 (B) in Table 1. The lower insets show the pattern of the polarized radiance PI of the fogbows. Along the bow the polarized radiance PI , the angular distance δ between the peaks of the primary bow and the first supernumerary bow, and the angular width σ of the primary bow change only moderately due to the small change of the droplet size. The directions ϕ (clockwise from the vertical) of the radii are given in the upper inset.

completely unpolarized due to the large scattering angles involved. For this reason the dilution (reduction) of the fogbow polarization is more extreme even though the scattered light has the same direction (angle) of polarization as the fogbow light.

Above the sea horizon, p of both the primary bow and first supernumerary of the fogbow is highest in the red spectral range [Figs. 2(f)–2(h) and 3(b)] and lowest in the blue [Figs. 2(h) and 3(d)]. The reason for this is that the radiance I of partly polarized skylight increases with decreasing wavelength λ , thus the background skylight dilutes progressively the fogbow light, which therefore results in a decrease in the net p (of fogbow light and skylight) with decreasing λ . Above the horizon the fogbow and its first

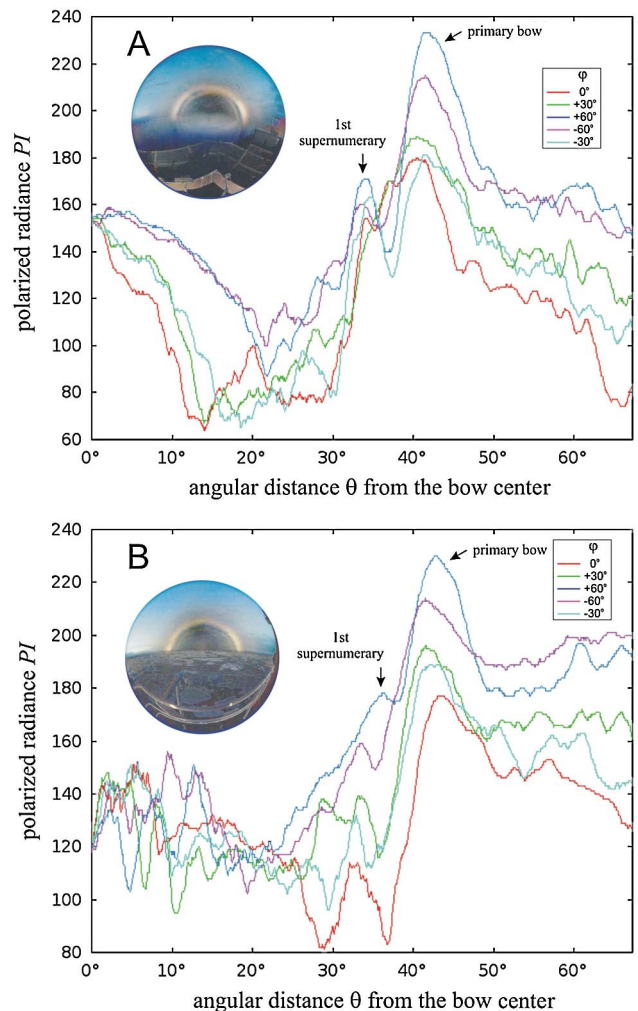


Fig. 5. (Color online) As Fig. 4 for the Arctic fogbows 7 (A) and 11 (B) in Table 1, along the bow of which the polarized radiance PI , the angular distance δ between the peaks of the primary bow and the first supernumerary bow, and the angular width σ of the primary bow change strongly due to the large change of the droplet size.

supernumerary are quite dark gray in the p patterns [Fig. 2(f)–2(h)] because both possess higher p values than the background sky. On the other hand, in the p patterns [Fig. 2(f)–2(h)] it is clearly seen that

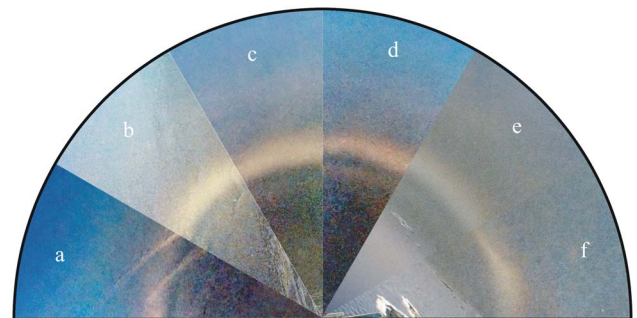


Fig. 6. (Color online) Comparison of six fogbows (a)–(f) in the pattern of polarized radiance PI measured in the high Arctic by imaging polarimetry.

the p values of the fogbow are quite low below the sea horizon. Thus, below the horizon, the fogbow and its first supernumerary are quite light gray (low p) relative to the dark gray (high p) sea surface. The reason for this is that the background light reflected from the sea surface is horizontally polarized, while the direction of polarization of fogbow light (being always tangential, i.e., parallel to the arc of the bow) below the horizon is obliquely or vertically polarized. Thus, the horizontally polarized water-reflected light reduces the polarization of the tangentially polarized fogbow light, resulting in a decrease in the net p . This also explains why in the PI pattern the fogbow is quite dark below the sea horizon, contrary to the bright whitish bow above the horizon [Fig. 2(b)].

The appearance of the 16 studied fogbows varied, that is the peak distance δ and the bow width σ changed more or less along their circular bow (Figs. 4–6, Table 1). The main reason for this variability could have been the spatiotemporal change of the droplet size within the fogbow. Two coauthors of this work, (S. Å. and G. H.) frequently observed that the appearance of a given Arctic fogbow changed drastically in time as the fog became denser/thinner, or the fog streamed turbulently as the observers were transported across the Arctic Ocean. This variability could be a consequence of the characteristics of the high Arctic: Open waters frequently occur in the ice shield resulting in a sudden spatial change of the droplet size within the fog at the water-ice margin. These spatial changes are temporally modulated by the changes due to atmospheric turbulency.

Figure 1 shows the simulated appearance of the fogbow as a function of the droplet diameter D ranging from 5 to 100 μm computed with the program IRIS developed by Les Cowley [23]. According to Fig. 1, both the peak distance δ and the bow width σ of the fogbow decreases with the increasing diameter D of the fog droplets. The value of D in fog changes both spatially and temporally in a chaotic manner due to the turbulence of air [32]. The angular extension of the primary fogbow is about $2 \times 42^\circ$. Within this angular region the distribution of droplet size can drastically change spatiotemporally, resulting in the diversity of the δ and σ values of the fogbows investigated by us (Table 1, Figs. 4–6).

We admit that the 180° field of view of the fisheye lens used in our imaging polarimeter was not ideal to study the fogbow, since it was too wide for the angular extension of $2 \times 52^\circ = 104^\circ$ of the fogbow including also the secondary bow. However, in the Beringia 2005 expedition, we used a full-sky (180° field of view) polarimeter because our major aim was to measure the celestial polarization patterns of the high Arctic under different sky conditions [33–37]. During this expedition we did not have a lens with a narrower field of view. Thus we had to measure with the only available 180° field-of-view lens.

Gábor Horváth thanks the German Alexander von Humboldt Foundation for an equipment donation. The Beringia 2005 expedition was organized by

the Swedish Polar Research Secretariat and Lund University, and the participation by Susanne Åkesson and Gábor Horváth was financed by a grant from the Swedish Research Council. Susanne Åkesson is also supported by a project grant from the Swedish Research Council and the Center for Animal Movement Research (CAnMove) financed by a Linnaeus grant (349-2007-8690) from the Swedish Research Council and Lund University. Ramón Hegedüs is a Marie Curie IEF fellow and he is grateful for the support of the European Commission. We are grateful to György Kriszka (Eötvös University, Biological Institute, Group for Methodology in Biology Teaching) for the digitization of the original color slides taken about Arctic fogbows through linear polarizers. We would like to express our thanks to Les Cowley for permission to use his IRIS Software to simulate the appearance of the fogbow as a function of the droplet size (Fig. 1). We thank two anonymous reviewers for their comments.

References

1. M. Minnaert, *Light and Color in the Open Air* (G. Bell and Sons, 1940).
2. J. V. Dave, "Scattering of visible light by large water spheres," *Appl. Opt.* **8**, 155–164 (1969).
3. R. A. R. Tricker, *Introduction to Meteorological Optics* (Elsevier, 1970).
4. R. Greenler, *Rainbows, Halos, and Glories* (Cambridge University, 1980).
5. R. L. Lee Jr and A. B. Fraser, *The Rainbow Bridge: Rainbows in Art, Myth, and Science* (Pennsylvania State University, 2001).
6. V. Khare and H. M. Nussenzveig, "Theory of the rainbow," *Phys. Rev. Lett.* **33**, 976–980 (1974).
7. S. D. Mobbs, "Theory of the rainbow," *J. Opt. Soc. Am.* **69**, 1089–1092 (1979).
8. H. M. Nussenzveig, "Complex angular momentum theory of the rainbow and the glory," *J. Opt. Soc. Am.* **69**, 1068–1079 (1979).
9. K. Sassen, "Angular scattering and rainbow formation in pendant drops," *J. Opt. Soc. Am.* **69**, 1083–1089 (1979).
10. S. D. Gedzelman, "Rainbow brightness," *Appl. Opt.* **21**, 3032–3037 (1982).
11. R. L. Lee, "What are 'all the colors of the rainbow'?" *Appl. Opt.* **30**, 3401–3407 (1991).
12. R. T. Wang and H. C. van de Hulst, "Rainbows: Mie computations and the Airy approximation," *Appl. Opt.* **30**, 106–117 (1991).
13. R. L. Lee, "Mie theory, Airy theory, and the natural rainbow," *Appl. Opt.* **37**, 1506–1519 (1998).
14. G. P. Können and J. H. de Boer, "Polarized rainbow," *Appl. Opt.* **18**, 1961–1965 (1979).
15. G. P. Können, *Polarized Light in Nature* (Cambridge University, 1985).
16. K. L. Coulson, *Polarization and Intensity of Light in the Atmosphere* (A. Deepak, 1988).
17. A. Barta, G. Horváth, B. Bernáth, and V. B. Meyer-Rochow, "Imaging polarimetry of the rainbow," *Appl. Opt.* **42**, 399–405 (2003).
18. G. Horváth and D. Varjú, *Polarized Light in Animal Vision—Polarization Patterns in Nature* (Springer-Verlag, 2004).
19. J. Tyndall, "Note on the white rainbow," *Philos. Mag.* **17**, 148–150 (1884).

20. J. C. McConnel, "The theory of fog-bows," *Philos. Mag.* **29**, 453–461 (1890).
21. K. Lenggenhager, "Ergänzungen zur Entstehung der Regenbogen, inneren Nebenbogen und Nebelbogen," *Arch. Met. Geoph. Biocl. A* **31**, 147–156 (1982).
22. D. K. Lynch and S. N. Futterman, "Ulloa's observation of the glory, fogbow, and an unidentified phenomenon," *Appl. Opt.* **30**, 3538–3541 (1991).
23. Cowley, "Software IRIS ©," (2011) <http://atoptics.co.uk>.
24. A. F. Hunter, "Rainbows, fogbows and their associated phenomena," *J. R. Astron. Soc. Can.* **15**, 345–358 (1921).
25. D. K. Lynch and P. Schwartz, "Rainbows and fogbows," *Appl. Opt.* **30**, 3415–3420 (1991).
26. K. von Bullrich, "Der Beginn der Nebelbildung und seine optische Auswirkung," *Zeitschrift für angewandte Mathematik und Physik* **14**, 434–441 (1963).
27. K. Lenggenhager, "Erklärung der im Vergleich zum Regen- und Nebelbogen umgekehrten Teilpolarisation der Nebelglorien," *Arch. Met. Geoph. Biocl. A* **32**, 165–172 (1983).
28. J. Gál, G. Horváth, A. Barta, and R. Wehner, "Polarization of the moonlit clear night sky measured by full-sky imaging polarimetry at full moon: comparison of the polarization of moonlit and sunlit skies," *J. Geophys. Res.* **106(D19)**, 22647–22653 (2001).
29. J. Gál, G. Horváth, V. B. Meyer-Rochow, and R. Wehner, "Polarization patterns of the summer sky and its neutral points measured by full-sky imaging polarimetry in Finnish Lapland north of the Arctic Circle," *Proc. R. Soc. A* **457**, 1385–1399 (2001).
30. I. Pomozi, G. Horváth, and R. Wehner, "How the clear-sky angle of polarization pattern continues underneath clouds: full-sky measurements and implications for animal orientation," *J. Exp. Biol.* **204**, 2933–2942 (2001).
31. G. Horváth, A. Barta, J. Gál, B. Suhai, and O. Haiman, "Ground-based full-sky imaging polarimetry of rapidly changing skies and its use for polarimetric cloud detection," *Appl. Opt.* **41**, 543–559 (2002).
32. T. E. W. Schumann, "Theoretical aspects of the size distribution of fog particles," *Q. J. R. Meteorol. Soc.* **66**, 195–208 (1940).
33. R. Hegedüs, S. Åkesson, and G. Horváth, "Polarization patterns of thick clouds: overcast skies have distribution of the angle of polarization similar to that of clear skies," *J. Opt. Soc. Am. A* **24**, 2347–2356 (2007).
34. R. Hegedüs, S. Åkesson, and G. Horváth, "Anomalous celestial polarization caused by forest fire smoke: Why do some insects become visually disoriented under smoky skies?" *Appl. Opt.* **46**, 2717–2726 (2007).
35. R. Hegedüs, S. Åkesson, R. Wehner, and G. Horváth, "Could Vikings have navigated under foggy and cloudy conditions by skylight polarization? On the atmospheric optical prerequisites of polarimetric Viking navigation under foggy and cloudy skies," *Proc. R. Soc. A* **463**, 1081–1095 (2007).
36. R. Hegedüs, S. Åkesson, and G. Horváth, "Polarization of "water-skies" above arctic open waters: how polynyas in the ice-cover can be visually detected from a distance," *J. Opt. Soc. Am. A* **24**, 132–138 (2007).
37. G. Horváth, A. Barta, I. Pomozi, B. Suhai, R. Hegedüs, S. Åkesson, V. B. Meyer-Rochow, and R. Wehner, "On the trail of Vikings with polarized skylight: Experimental study of the atmospheric optical prerequisites allowing polarimetric navigation by Viking seafarers," *Phil. Trans. R. Soc. B* **366**, 772–782 (2011).